Investigation of the mechanical properties and porosity relationships in fused deposition modelling-fabricated porous structures

Ker Chin Ang, Kah Fai Leong and Chee Kai Chua
School of Mechanical and Production Engineering, Nanyang Technological University, Singapore, and

Margam Chandrasekaran
Singapore Institute of Manufacturing Technology, A*Star, Singapore

Abstract

Purpose – The purpose of this paper is to investigate the mechanical properties and porosity relationships in fused deposition modelling (FDM) fabricated porous structures.

Design/methodology/approach – Porous structures of numerous build architectures aimed at tissue engineering (TE) application were fabricated using the FDM. The employment of FDM to fabricate these non-random constructs offers many advantages over conventional scaffold fabrication techniques as patient specific scaffolds with well-defined architectures and controllable pore sizes can be fabricated accurately and rapidly. There exist several FDM parameters that one needs to specify during the scaffold fabrication process. These parameters, which can be interdependent and exhibit varying effects on scaffold properties, were identified and examined using the design of experiment (DOE) approach. Essentially, the effects of five FDM process parameters, namely air gap, raster width, build orientation, build layer and build profile, on the porosity and mechanical properties of acrylonitrile-butadienene-styrene (ABS) scaffold structures with three-dimensional interconnectivity were investigated in two designed experiments. Statistical analyses of the data were performed and the respective factors that have significant influence on the porosity and mechanical properties of the scaffolds were identified. The relationship between scaffold's mechanical properties and porosity was thereafter established empirically.

Findings – Models of TE scaffolds of numerous build architectures were successfully fabricated using different parameter settings on the FDM. The DOE approach determined air gap and raster width as the most significant parameters in affecting the porosity and mechanical properties of the ABS scaffold structures. The relationship between scaffolds' mechanical properties and porosity was determined to be logarithmic, with the best mechanical properties observed in scaffolds of low porosity.

Originality/value – The paper highlights how the application FDM to tissue scaffold application can overcome most of the limitations encountered in the conventional techniques.

Keywords Rapid prototypes, Porous materials, Modelling

Paper type Research paper

1. Introduction

Tissue engineering (TE) is an emerging interdisciplinary field that involves the application of engineering principles to create devices for the study, restoration, modification, and assembly of functional tissues from native or synthetic sources (Williams, 1999). Most TE approaches towards creating functional replacement tissues or organs utilise temporary porous scaffolds to guide the proliferation and differentiation of seeded cells *in vitro* and *in vivo* as well as to provide for the mechanical stability of the biological substitutes in a three-dimensional organisation. The design and development of TE scaffolds is thus currently one of the most intensively investigated aspects of TE.

Currently, a variety of conventional techniques are available for the fabrication of tissue scaffolds (Leong *et al.*, 2003; Thomson *et al.*, 2000). However, much of these techniques have serious shortcomings that restrict their scope of applications. Inconsistency in pore size reproduction, irregularity in pore distribution, indispensible usage of toxic organic solvents, labour-intensive and deficiency in scaffolds' mechanical strength are some of the problems commonly associated with these fabrication techniques (Yang *et al.*, 2001; Sachlos and Czernuszka, 2003).

The application of fused deposition modelling (FDM) to tissue scaffold fabrication aims to overcome most of the limitations encountered in the conventional techniques. Essentially, FDM is a material deposition process, which has the capability to create physical three-dimensional objects from a CAD solid model via computer-controlled robotic

The current issue and full text archive of this journal is available at
www.emeraldinsight.com/1355-2546.htm

Rapid Prototyping Journal
12/2 (2006) 100–105
© Emerald Group Publishing Limited [ISSN 1355-2546]
[DOI 10.1108/13552540610652447]

The authors express their appreciation to Singapore Polytechnic for the use of its FDM machine for this research.

Received: 1 June 2005
Revised: 1 July 2005
Accepted: 29 November 2005

extrusion of thin rods of polymeric materials (Chua *et al.*, 2003). FDM allows the computerized fabrication of tissue scaffolds requiring only minimal manpower. This computer-controlled process not only allow complex scaffolds of varied designs to be realised, it also makes possible the customisation of patient specific implants and offers ease and flexibility in controlling scaffold characteristics to suit the structural and functional needs in different TE applications. Also, with the relatively high build resolution of FDM and its abilities to define and control individual process parameters, the technique has the ability to provide excellent control over scaffold external shape and internal pore interconnectivity and geometry. Last but not least, the FDM process does not require the use of toxic chemicals and porogens in tissue scaffold fabrication (Leong *et al.*, 2003; Yang *et al.*, 2002).

FDM has been employed in the fabrication of polycaprolactone (PCL) scaffolds with honeycomb-like pattern, fully interconnected channel network, and controllable porosity (Zein *et al.*, 2002). By varying FDM process parameters, scaffolds of varied porosity and mechanical properties were achieved. The *in vitro* cell cultural response of primary human fibroblast and periosteal cells on FDM-fabricated PCL scaffolds has also been investigated (Hutmacher *et al.*, 2002). The results demonstrated favourable cell cultural response and good mechanical properties of FDM-processed biopolymer. The development and fabrication of polypropylene-tricalcium phosphate scaffolds using the FDM was also reported (Kalita *et al.*, 2003). While compressive testings showed that scaffold strength decreased with increasing pore volume, cytotoxicity and cell proliferation studies revealed that the FDM-fabricated scaffolds were non-toxic and promoted cell growth.

There exist numerous parameters that one needs to specify during the fabrication process in order to produce porous structures of the desired properties. These parameters can be interdependent and they affect the properties of the constructs in varying degree (Agarwala *et al.*, 1996; Ahn *et al.*, 2002; Montero *et al.*, 2001; Weinmann *et al.*, 2003). It was the objective of the project to determine the effects of some of these FDM process specific parameters. Through the use of the design of experiment (DOE) approach, the porosity and mechanical properties of FDM-fabricated acrylonitrile-butadienene-styrene (ABS) scaffolds (the standard FDM build material, ABS P400, was chosen instead of a bioresorbable material to reduce the number of material specific variables, which were not optimised for the FDM process) were examined in two designed experiments as five process parameters, namely, air gap, raster width, build profile, build orientation and build layers, were systematically varied.

2. Experimental methodology and equipment

In the first experiment, a two-level fractional factorial (2^{k-1}) DOE, as shown in Figure 1, screened samples fabricated from 16 different build conditions for the most significant process parameters affecting porosity and mechanical properties. After raster width and air gap had been established as the two most important parameters, a five-level factorial designed experiment was next set-up to investigate their effects on scaffolds' properties with more accuracy.

To identify the process parameters that most significantly influence the porosity and mechanical properties of the scaffolds, the analysis of variance method was used in conjunction with the *F*-distribution (upper-tailed, 95 per cent) (Montgomery, 1996). Empirical models based on the results were subsequently formulated to relate the scaffolds' porosity to their mechanical properties.

ABS samples used in the study were fabricated using the Stratasys' FDM 1650 machine. All samples were built having dimensions of 12.5 mm (diameter) by 25 mm (height) as specified by the ASTM compressive testing method D695-02a (ASTM, 2002). ABS filaments (of diameter 1.78 mm) under the trade name of ABS P400 were supplied by Stratasys Incorporated.

The Quantachrome Instruments' ultrapycnometer (Ultrapycnometer 1000) was used to measure the porosity of FDM-fabricated ABS scaffolds. A maximum standard deviation value of 0.01 per cent was preset. The method allowed the determination of the cellular volume (V_1) of the scaffolds and the porosity was calculated from the formula given in ASTM D2856-94 (ASTM, 1994):

$$P_{pyc} = \left(\frac{V - V_1}{V}\right) \times 100 \text{ per cent} \qquad (1)$$

where P_{pyc} is the porosity of the scaffold measured using the ultrapycnometer and V is the geometric volume of the specimen.

The mechanical properties of the samples were investigated on the Instron 5569 machine (Instron Corporation). Based on the standard compressive test method specified by ASTM D695-02a, five samples of each treatment combination were tested at a test speed of 1 mm/min and a 10 kN load cell was used. The test data were collected by Instron's Merlin Software (Series 5500).

3. Results and discussions

3.1 Determination of the significant process parameters via a two-level fractional factorial designed experiment

The results of this experiment, which have been previously presented in details by Ang *et al.* (2004), are summarised here. The compressive strength of the sample was defined as the maximum compressive stress carried by the test specimen during the test whereas the compressive modulus of elasticity, or simply compressive modulus, was calculated as the ratio of stress to the corresponding strain below the proportional limit of the material. The experiment was aborted only after a strain of at least 20 per cent was recorded.

3.1.1 Porosity measurements

The porosity measurement results revealed that a wide range of scaffolds with different porosities could be fabricated using the FDM technique. The scaffolds have porosity values that ranged from 14.7 to 84.8 per cent. Statistical analysis of the experimental results (P_{pyc}) determined that only the two main effects of air gap (A) and raster width (B) and the interaction between air gap and raster width (AB) affected the porosity of the scaffolds significantly. On the other hand, build orientation (C), build laydown pattern (D), build layer (E), and other interaction effects, were found not to have significant effect on porosity.

Air gap had the largest effect on porosity of a scaffold. On average, a change in air gap value from 0 mm (-1) to 1.27 mm ($+1$) caused the porosity of the sample to increase 51.32 per cent. In contrast, raster width was found to affect

Figure 1 FDM process parameters illustrated at both low- and high-levels

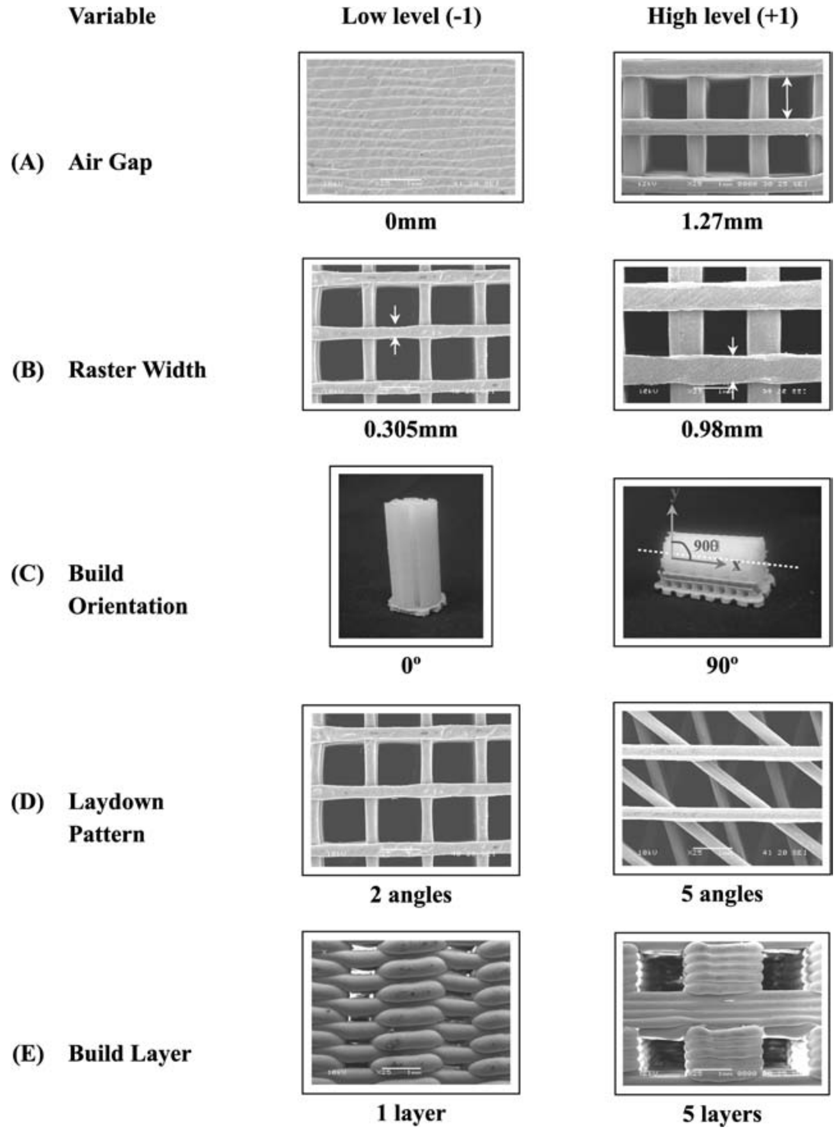

porosity in the opposite manner. A change in raster width value from 0.305 mm (-1) to 0.98 mm ($+1$) caused, on average, a 16.74 per cent decrease in porosity. The highest porosity was achieved when the scaffolds were fabricated using a setting combination of low (-1) raster width and high ($+1$) air gap.

3.1.2 Scaffold's mechanical properties

The averaged results from the experiments, which included the compressive strength and compressive modulus of the porous samples, are presented in Table I.

Compressive stress for the 16 different samples investigated ranged from 0.71 to 47.93 MPa whereas the measured compressive modulus ranged between 28.52 and 988.03 MPa. Generally, it was found that samples having low compressive modulus possess low strength as well. Statistical analysis of the experimental data revealed that the main effect, air gap (A), raster width (B) and build orientation (C) and the interaction between build laydown pattern and build layer (DE) influenced the compressive strength of the scaffolds significantly. It was determined from the analysis that air gap had the largest effect on the compressive strength of the scaffolds. A change in air gap value from 0 to 1.27 mm caused a mean decrease in strength of the specimens by 35.13 MPa. On the other hand, a change in the raster width value from 0.305 to 0.98 mm was found to have increased the compressive strength of the scaffolds by 7.8 MPa. Changes in both build orientation and the interaction between build laydown pattern and build layer from a low-level (-1) to a high-level ($+1$) setting was found to have decreased the strength of the scaffolds by 4.83 and 5.28 MPa, respectively.

It was determined that the compressive modulus of the scaffolds was only affected by two main effects – air gap and raster width. It was revealed that air gap had the largest effect on the compressive strength of the scaffolds. A change in air gap value from no air gap (0 mm) to 1.27 mm caused a mean decrease in the compressive modulus of the specimens by 586 MPa. In contrast, a change in the raster width value from 0.305 to 0.98 mm was found to increase the compressive

Rapid Prototyping Journal
Volume 12 · Number 2 · 2006 · 100–105

Table I The two-level fractional factorial (2^{5-1}) design layout

Factor	Name						− 1 level	+1 level
A	Air gap						0	1.27
B	Raster width						0.305	0.98
C	Build orientation						Transverse (0°)	Axial (90°)
D	Build laydown pattern						2 angles	5 angles
E	Build layer						2	5
Run	*A*	*B*	*C*	*D*	*E*	*Strength (MPa)*	*Modulus (MPa)*	*Porosity (per cent)*
1	−	−	−	−	+	42.62	488.07	23.5
2	+	−	−	−	−	2.47	63.36	82.9
3	−	+	−	−	−	47.93	968.80	8.5
4	+	+	−	−	+	13.61	271.49	51.9
5	−	−	+	−	−	32.07	988.03	20.6
6	+	−	+	−	+	0.71	50.60	82.6
7	−	+	+	−	+	44.53	757.18	12.2
8	+	+	+	−	−	7.40	201.61	56.6
9	−	−	−	+	−	47.19	387.32	19.7
10	+	−	−	+	+	0.99	49.83	80.8
11	−	+	−	+	+	38.74	660.37	8.8
12	+	+	−	+	−	16.62	130.80	51.5
13	−	−	+	+	+	31.59	681.67	21.2
14	+	−	+	+	−	1.01	28.52	81.1
15	−	+	+	+	−	45.68	767.03	7.6
16	+	+	+	+	+	7.55	214.51	53.5

modulus of the scaffolds by 154 MPa. No interaction effect was determined to influence the compressive modulus in any significant manner statistically.

3.2 Investigation of the effects of raster width and air gap on properties of ABS scaffolds via a five-level factorial designed experiment

While the two-level fractional factorial DOE has established that the FDM process parameters of raster width and air gap have greater effects on the scaffolds' properties (porosity and mechanical properties) than the other process parameters, results obtained from the experiment were generally not precise enough to estimate the scaffolds' properties for other levels that were not investigated. As such, a five-level factorial designed experiment was set-up to investigate the effects of raster width and air gap on scaffolds' properties with more accuracy. The five levels of raster width chosen were 0.305, 0.580, 0.730, 0.830 and 0.980 mm while air gap assumed the five levels of 0.127, 0.305, 0.730, 0.980 and 1.270 mm. In all, 25 treatment combinations of ABS scaffolds were fabricated and tested.

3.2.1 Porosity measurements

The highest average porosity of 83.1 per cent was observed in scaffolds built having a raster width and air gap combination of 0.305 and 1.27 mm, respectively , while scaffolds having a raster width – air gap combination of 0.98 and 0.127 mm exhibited the least porosity (25.6 per cent). Generally, it can be observed from Table II that porosity decreased as raster width increased as well as when air gap decreased.

A quadratic regression model that relates the process parameters of air gap and raster width to scaffolds' porosity was derived from the data empirically (Montgomery, 1996).

$$\text{Porosity} = 54.1 + 66.5G_{\text{air}} - 58.9W_{\text{raster}} - 20.2G_{\text{air}}^2 + 23.3W_{\text{raster}}^2 - 13.1G_{\text{air}}W_{\text{raster}} \quad (2)$$

where G_{air} is the air gap in mm and W_{raster} is the raster width in mm.

The accuracy of the empirical model was tested by comparing the porosity values obtained by equation (2) with the actual experimental data and the results showed that the overall deviation averaged 1.9 per cent with a single largest deviation of 5.5 per cent.

3.2.2 Scaffold's mechanical properties

Compressive tests for all the samples in the experiments were conducted in the same manner as described in Section 3.1.2. The use of offset compressive yield strength as a measurement of the material strength instead of compressive strength was necessary as some of the samples did not exhibit a maximum peak on the stress-strain diagram for the range investigated. In this project, the offset compressive yield strength of the material was defined as the stress at which stress-strain curve departs from linearity by 2 per cent of deformation (strain). Table II summarises the average offset compressive yield strength and the compressive modulus of the scaffolds with the 25 treatment combinations alongside their respective porosity for comparison.

Offset compressive yield strength for the 25 different samples investigated was found to vary from 1.31 to 31.28 MPa while compressive modulus ranged between 34.0 and 967.7 MPa. The highest offset compressive yield strength and compressive modulus were observed in scaffolds built having a raster width and air gap combination of 0.98 and 0.127 mm, respectively. On the other hand, scaffolds fabricated having a raster width and air gap combination of 0.305 and 1.27 mm, respectively , displayed the lowest mechanical properties. As can also be noted from Table II, the best mechanical properties were observed in scaffolds with the least porosity and vice versa.

Using the results of Table II, the relationship between scaffolds' offset compressive yield strength and their

Rapid Prototyping Journal
Volume 12 · Number 2 · 2006 · 100–105

Table II Comparisons of compressive yield strength and modulus against scaffolds' porosity

Air gap/raster width (mm/mm)	Porosity (per cent)	Offset compressive yield strength (MPa)	Compressive modulus (MPa)
0.127/0.305	35.67	23.14	748.8
0.127/0.580	34.79	24.03	769.4
0.127/0.730	30.91	28.21	890.8
0.127/0.830	27.45	29.49	937.8
0.127/0.980	25.63	31.28	967.7
0.305/0.305	62.27	5.59	126.8
0.305/0.580	47.04	14.60	343.2
0.305/0.730	40.29	20.61	567.6
0.305/0.830	34.96	24.83	690.9
0.305/0.980	36.9	26.43	742.3
0.730/0.305	77.34	2.62	52.3
0.730/0.580	61.73	8.99	54.5
0.730/0.730	53.2	15.24	277.4
0.730/0.830	51.83	17.61	432.2
0.730/0.980	49.16	19.82	458.3
0.980/0.305	80.07	2.03	55.4
0.980/0.580	66.16	6.75	64.3
0.980/0.730	54.52	15.66	358.9
0.980/0.830	51.67	18.59	485.2
0.980/0.980	48.28	20.22	548.2
1.27/0.305	83.1	1.31	34.0
1.27/0.580	69.59	5.94	60.8
1.27/0.730	66.06	9.89	168.0
1.27/0.830	62.15	13.37	217.0
1.27/0.980	57.1	16.04	399.1

respective porosity is plotted in Figure 2. Curve-fitting was performed for the experimental data and the variation of offset compressive yield strength, σ_c, with porosity was found to fit a logarithmic curve with the equation:

$$\sigma_c = -25.8 \ln P + 116.9 \quad (3)$$

where P is the per cent porosity of the scaffolds.

Similarly, the relationship between scaffolds' compressive modulus and their respective porosity is plotted in Figure 3. Curve-fitting was again performed and the variation of compressive modulus, E_c, with porosity (P) was found to fit a logarithmic curve with the equation:

$$E_c = -886.9 \ln P + 3879.8 \quad (4)$$

Figure 2 Effect of porosity on offset compressive yield strength of FDM scaffolds

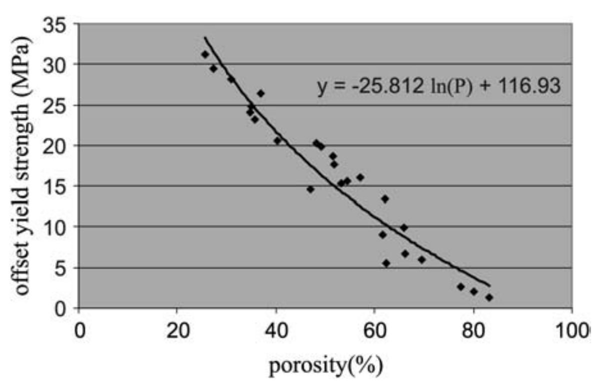

The establishment of both equations is very useful in that it allows the approximation of the scaffold's strength given its porosity and vice versa.

4. Conclusion

Models of TE scaffolds of numerous build architectures were successfully fabricated using different parameter settings on the FDM. The DOE approach determined air gap and raster width as the most significant parameters in affecting the porosity and mechanical properties of the ABS scaffold structures. The relationship between scaffolds' mechanical properties and porosity was determined to be logarithmic, with the best mechanical properties observed in scaffolds of low porosity.

Figure 3 Effect of porosity on compressive modulus of FDM scaffolds

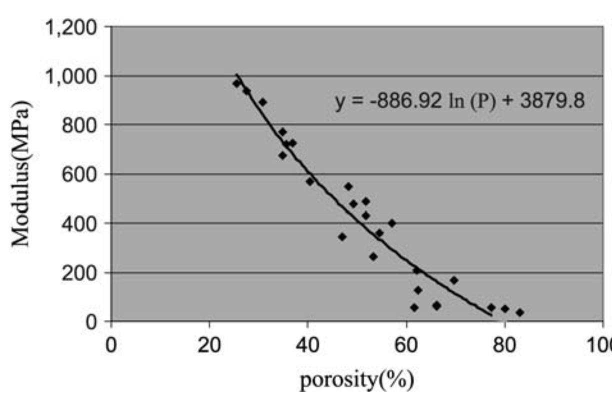

References

Agarwala, M.K., Jamalabad, V.R., Langrana, N.A., Safari, A., Whalen, P.J. and Danforth, S.C. (1996), "Structural quality of parts processed by fused deposition", *Rapid Prototyping Journal*, Vol. 2 No. 4, pp. 4-19.

Ahn, S.H., Montero, M., Odell, D., Roundy, S. and Wright, P.K. (2002), "Anisotropic material properties of fused deposition modelling ABS", *Rapid Prototyping Journal*, Vol. 8 No. 4, pp. 248-57.

American Society for Testing and Materials (1994), "Standard test method for open-cell content of rigid cellular plastics by air pycnometer, D2856-94", ASTM, West Conshohocken, PA.

American Society for Testing and Materials (2002), "Standard test method for compressive properties of rigid plastics, D695-02a", ASTM, West Conshohocken, PA.

Ang, K.C., Leong, K.F. and Chua, C.K. (2004), "Investigation of non-random fused deposition modelling-fabricated three dimensional porous structures by designed experiment", *Proceedings, the Sixth International Conference on Frontiers of Design and Manufacturing, Xian, China*, 20-23 June.

Chua, C.K., Leong, K.F. and Lim, C.S. (2003), *Rapid Prototyping: Principles and Applications*, 2nd ed., World Scientific Publishing Co., Singapore.

Hutmacher, D.W., Schantz, T., Zein, I., Ng, K.W., Teoh, S.H. and Tan, K.C. (2002), "Mechanical properties and cell cultural response of polycaprolactone scaffolds designed and fabricated via fused deposition modelling", *Journal of Biomedical Material Research*, Vol. 55, pp. 203-16.

Kalita, S.J., Bose, S., Hosick, H.L. and Bandyopadhyay, A. (2003), "Development of controlled porosity polymer-ceramic composite scaffolds via fused deposition modeling", *Materials Science & Engineering*, Vol. 23, pp. 611-20.

Leong, K.F., Cheah, C.M. and Chua, C.K. (2003), "Solid freeform fabrication of three-dimensional scaffolds for engineering replacement tissues and organs", *Biomaterials*, Vol. 24, pp. 2363-78.

Montero, M., Odell, D., Roundy, S., Ahn, S.H. and Wright, P.K. (2001), "Material characterization of fused deposition modeling (FDM) process", *Proceedings, Rapid Prototyping and Manufacturing Conference, Society of Manufacturing Engineers, Cincinnati, Ohio*, 15-17 May.

Montgomery, D.C. (1996), *Design and Analysis of Experiments*, 4th ed., Wiley, New York, NY.

Sachlos, E. and Czernuszka, J.T. (2003), "Making tissue engineering scaffolds work. Review on the application of solid freeform fabrication technology to the production of tissue engineering scaffolds", *European Cells and Materials*, Vol. 5, pp. 29-40.

Thomson, R.C., Shung, A.K., Yaszemski, M.J. and Mikos, A.G. (2000), "Polymer scaffold processing", in Lanza, R.P. *et al.* (Eds), *Principles of Tissue Engineering*, 2nd ed., Academic Press, London, pp. 251-62.

Weinmann, J., Ip, H., Prigozhin, D., Escobar, E., Mendelson, M. and Noorani, R. (2003), "Application of design of experiments (DOE) on the processing of rapid prototyped samples", *The Solid Freeform Symposium, Proceedings, Austin, Texas*, pp. 340-7, 4-6 August.

Williams, D.F. (1999), *The Williams Dictionary of Biomaterials*, Liverpool University Press, Liverpool, p. 318.

Yang, S.F., Leong, K.F., Du, Z.H. and Chua, C.K. (2001), "The design of scaffolds for use in tissue engineering. Part 1. Traditional factors", *Tissue Engineering*, Vol. 7 No. 6, pp. 679-89.

Yang, S.F., Leong, K.F., Du, Z.H. and Chua, C.K. (2002), "The design of scaffolds for use in tissue engineering. Part 2. Rapid prototyping techniques", *Tissue Engineering*, Vol. 8 No. 1, pp. 1-11.

Zein, I., Hutmacher, D.W., Tan, K.C. and Teoh, S.H. (2002), "Fused deposition modelling of novel scaffold architectures for tissue engineering applications", *Biomaterials*, Vol. 23, pp. 1169-85.

Corresponding author

Kah Fai Leong can be contacted at: mkfleong@ntu.edu.sg